



AM1 Study of *N*-2-Acetylaminofluorene bonded to Deoxyguanosine at the Minor Adduct Site

M. BESSON^{1,*} and E.P. BATCHELOR^{1,2}

¹Department of Physics, Villanova University, Villanova, Pennsylvania 19085, USA

²Department of Physics and Astronomy, University of Pennsylvania, Philadelphia, Pennsylvania 19104, USA

(*Author for correspondence, e-mail: mbesson@villanova.edu)

Abstract. We have computed the total energy as a function of six important torsion angles of the carcinogen *N*-2-acetylaminofluorene (AAF) bonded to the nitrogen N2 of deoxyguanosine using the semiempirical quantum mechanical method AM1. One global minimum and one local minimum are found separated by a modest barrier. We have computed the normal-mode frequencies of the relevant torsional motions and have determined the rate of conversion between the two minima.

Key words: deoxyguanosine, *N*-2-acetylaminofluorene, AAF, carcinogen, AM1

1. Introduction

During the last four decades the carcinogenic effect of aromatic amines has been firmly established experimentally. These substances are found in the environment and are produced by automobile exhaust, tobacco smoke, and chemical dyes. In a study funded by the U.S. Environmental Protection Agency, nearly 50 aromatic amines tested positive for carcinogenicity [1]. A wide variety of experimental and theoretical studies on these agents have been made in the last 30 years, and it is widely accepted that the origin of chemical carcinogenesis is the covalent binding to DNA.

Much attention has been given to *N*-2-acetylaminofluorene (AAF) bonded to DNA which has been observed *in vitro* [2, 3, 4, 5, 6, 7, 8, 9, 10] and *in vivo* [11, 12, 13]. Generally these interactions produce mutations in the form of transversions and transitions of the base pairs. In about 85 percent of the cases the bonding occurs between the carbon C8 of the guanosine and the nitrogen N2 of AAF. It has been observed that this bonding is accompanied by the insertion of AAF between adjacent bases resulting in base pair rupturing [14, 15, 16, 17]. Computational studies have been undertaken on AAF-modified guanosine and other modified base polymers using the semiclassical molecular mechanics [18, 19, 20, 21, 22] as well as semiempirical quantum mechanics [23].

In the remaining instances the bond is formed between the nitrogen N2 of the guanosine and the carbon C3 of AAF. This minor adduct is believed to be important in carcinogenesis because it has been shown to persist in mammals and is repaired more slowly compared to the major adduct. It is not digested by S1 nuclease suggesting that base pairing is not disrupted. Early models showed that the fluorenyl moiety could lie in either the major or minor groove of B-DNA with little or no distortion. A recent molecular mechanics and dynamics analysis predicted several stable minor-groove conformations [24].

In the present study, we have explored the interaction of the minor adduct of AAF with deoxyguanosine and have obtained the total energy of the system as a function of six important torsion angles. This is accomplished by a quantum mechanical semiempirical molecular orbital approach, the Austin Model 1 (AM1) method. We have located two stable low energy configurations, and have calculated the energetics of the conversion between them.

2. Computational Method

The environment of the DNA interaction site is simulated by a finite cluster of atoms terminated with hydrogen atoms. The 60-atom cluster is composed of deoxyguanosine bonded at the nitrogen N2 with the carbon C3 of AAF. The initial geometries of the two moieties were obtained from standard published data [25], and from X-ray and NMR studies [26]. The cluster is shown in Figure 1. Six torsion angles α , β , γ , δ , ϵ and χ are also shown.

To investigate the energy surface in configuration space of this cluster we have used the AM1 method [27] provided in the software package MOPAC 6 [28]. AM1 is a semiempirical self-consistent implementation of the Hartree-Fock-Roothaan equations based on the NDDO (neglect of differential diatomic overlap) approximation. The molecular wave function is constructed as a linear combination of atomic orbitals, and the Hamiltonian matrix elements are parameters which have been previously determined from molecular data. Three- and four-center integrals are set to zero, and the remaining one- and two-center terms depend on adjustable parameters. These parameters have been obtained from experimental data on many small molecules such as bond lengths, heats of formation, and dipole moments. The AM1 method produces reliable total energies as a function of atomic positions and is able to probe the energy surface to find the minimum energy configurations. AM1 represents a significant improvement over earlier NDDO methods (such as MNDO [29]) especially in its ability to predict physically reasonable hydrogen bonds.

As an initial check of consistency, the geometry of each of the two moieties was determined by minimizing the total energy separately, allowing all bond lengths and angles to relax. This produced insignificant changes in energy and arrangement from the published data. The final molecule was then assembled by joining the nitrogen N2 of the deoxyguanosine with the carbon C3 of the AAF.

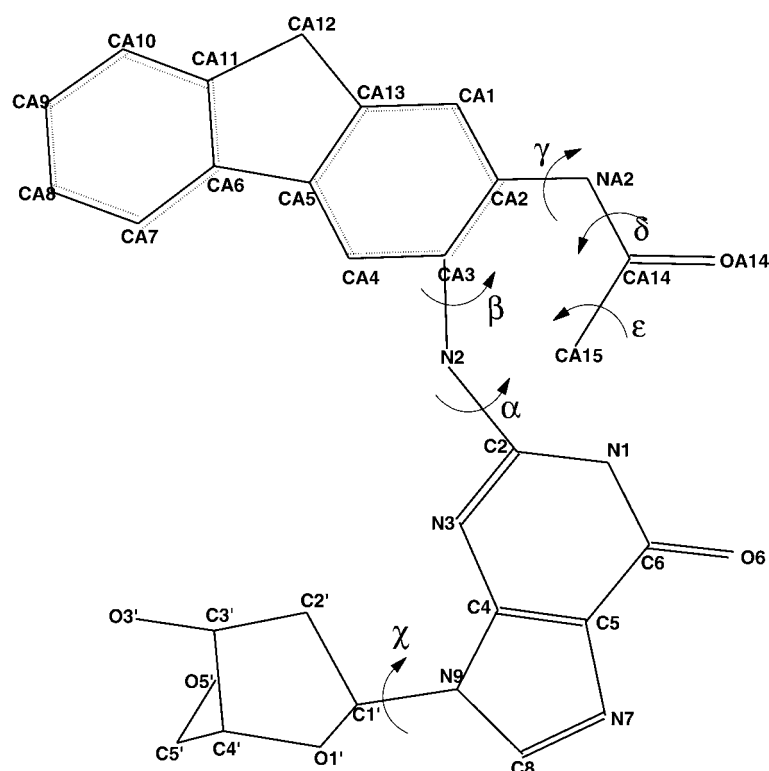


Figure 1. Representation of the DNA interaction site. Hydrogen atoms are not shown. The torsion angles are: α : N1-C2-N2-CA3; β : C2-N2-CA3-CA2; γ : CA3-CA2-NA2-CA14; δ : CA2-NA2-CA14-CA15; ϵ : NA2-CA14-CA15-H; χ : O1'-C1'-N9-C4.

A series of starting geometries was used in which the torsion angles β and χ occupied points on a grid of frequency 15° in each direction. The other four torsion angles α , γ , δ , and ϵ were initialized to arbitrary values. The sugar pucker was fixed in the C2'-endo configuration as is found in B-DNA. Obvious symmetry constraints were imposed, such as keeping the dihedral angles of the methyl hydrogens 120° apart when rotating ϵ . All geometry optimization was done with the Davidon-Fletcher-Powell minimization algorithm [30, 31], and along each path to the final configuration the values of the total energy and the six torsion angles were recorded. Each minimization path was checked manually. In some instances, the minimization algorithm proceeded along a path of slightly higher energy. This usually occurred at points where the angle α changed abruptly. In these cases the paths were recalculated starting with values of α , γ , δ , and ϵ rotated 180° from the initial trial. Thus a thorough map of the β - χ energy surface was obtained.

Local modes of vibration for two torsion angles were also computed using AM1. After energy minimization, the matrix of second derivatives of the energy with respect to rotations of these angles (the Hessian) was calculated. The mass-

Table I. Equilibrium geometries from AM1. The torsion angles are defined in Figure 1

Heat of formation (kcal/mol)	α	χ	β	γ	δ	ϵ
-23.15	177.8°	230.4°	88.2°	245.7°	179.6°	0.4°
-20.70	181.0°	225.7°	249.1°	96.4°	-0.3°	0.2°

weighted eigenvalues and eigenvectors of this matrix produce the normal-mode frequencies and displacements.

3. Results and Discussion

Starting from initial values of the torsion angles which covered all of configuration space, we performed a series of AM1 calculations on the dG-AAF entity. At each point along the energy minimization, the values of the energy and angles were recorded, producing a complete map of the energy surface. In a few cases, steric interactions prevented the determination of a final equilibrium geometry. Except for these, the system relaxed into one or the other of two minimum energy configurations. Although repulsive H-H interactions have been known to produce artificial stable configurations in AM1 [27], the shortest distance of 2.4 Å occurs between the hydrogen atoms on the nitrogens N1 and N2 of both stable configurations, acceptably above the critical value of 1.8–2.2 Å.

For the absolute minimum, the computed heat of formation was found to be -23.15 kcal/mol. The other stable minimum was found to have a heat of formation of -20.70 kcal/mol. The equilibrium values of the torsion angles are shown in Table I. The spatial geometries for the two minima are shown in Figure 2.

The results of our calculations show two well-defined and localized minima of the total energy surface. In moving away from either well the energy increases monotonically. There are no other shallow local minima anywhere on the surface. There is a modest energy ridge between the minima located approximately along $\beta = 180^\circ$ and a much higher barrier at $\beta = 0^\circ$. The minima are somewhat flat through an area about 30° on a side.

Investigation of the energy surface revealed that the total energy is most sensitive to variations in the angle β which according to Figure 1 is reasonable. To study the conversion of the molecule between the two minima, we performed a reaction-path calculation as a function of β . The other five torsion angles were allowed to relax along each point of the path. The total energy as a function of the reaction coordinate is shown in Figure 3, which shows the energy difference between the minima to be 2.45 kcal/mol and the barrier height to be $\Delta E_b = 5.93$ kcal/mol as measured from the lower minimum.

The torsion angle α changes monotonically with β throughout most of the path. However, there is an abrupt change from $\alpha = 96.9^\circ$ to $\alpha = 266.9^\circ$ near $\beta =$

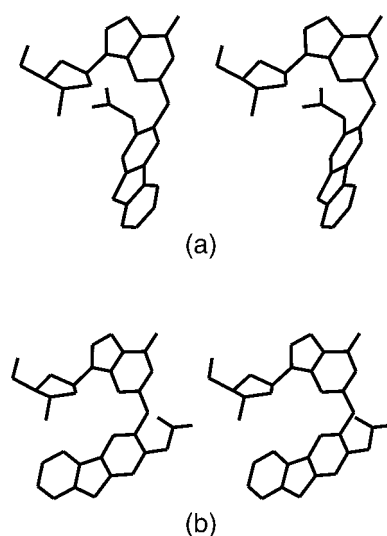


Figure 2. Stereograms of the dG-AAF minor adduct calculated from AM1. Hydrogen atoms are not shown. (a) Lowest energy configuration; (b) local minimum 2.45 kcal/mol higher in energy.

180°, which is the position of the energy barrier between minima. In this region the methyl group on the AAF begins approaching the sugar and the energy increase starts becoming appreciable. The variation of α along the reaction path is shown in the upper part of Figure 3.

The relative equilibrium populations of the two minima can be found from the Boltzmann probability distribution: $P_2/P_1 = \exp[-(E_2 - E_1)/kT]$, where k is Boltzmann's constant, T is the temperature, and $E_2 - E_1$ is the energy difference between the minima. For $T = 310$ K, and $E_2 - E_1 = 2.45$ kcal/mol, we find $P_2/P_1 = 0.019$.

To study the dynamics near the minimum, we investigated the local rotational modes associated with α and β . MOPAC 6 provides a means to find normal modes by first relaxing all bond lengths and angles and then calculating all the modes. Since we wanted the deoxyguanosine structure to maintain its form and were interested in the local α - β vibrations only, we performed the analysis directly from first principles.

We start with a Lagrangian $L = T - V$. The kinetic energy is

$$T(\dot{\theta}_1, \dot{\theta}_2, \dot{\theta}_3, \dot{\theta}_4) = \frac{1}{2}I_1\dot{\theta}_1^2 + \frac{1}{2}I_2\dot{\theta}_2^2 + \frac{1}{2}I_3\dot{\theta}_3^2 + \frac{1}{2}I_4\dot{\theta}_4^2, \quad (1)$$

where a dot above a coordinate indicates the total time derivative. The angles θ_i and the moments of inertia I_i are defined in Figure 4.

The potential energy is a function of α and β , and is written in the harmonic approximation about the minimum as

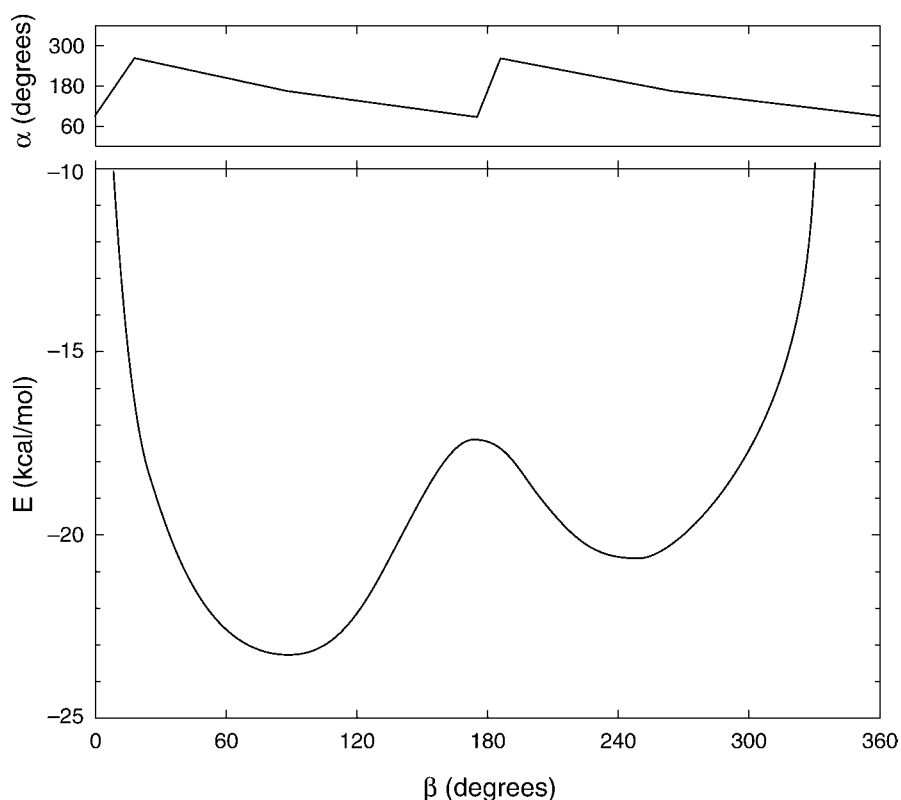


Figure 3. Reaction path between the two minima showing the total energy as a function of the torsion angle β . The energy difference between minima is 2.45 kcal/mol, and the barrier height from the global minimum is $\Delta E_b = 5.93$ kcal/mol. The upper plot shows the torsion angle α which changes abruptly near the top of the barrier.

$$V(\alpha, \beta) =$$

$$V(\alpha_0, \beta_0) + \frac{1}{2}V_{\alpha\alpha}(\alpha - \alpha_0)^2 + V_{\alpha\beta}(\alpha - \alpha_0)(\beta - \beta_0) + \frac{1}{2}V_{\beta\beta}(\beta - \beta_0)^2, \quad (2)$$

where α_0 and β_0 are the equilibrium values, and the coefficients are given by

$$V_{\mu\nu} = \left. \frac{\partial^2 V}{\partial \mu \partial \nu} \right|_{\substack{\alpha=\alpha_0 \\ \beta=\beta_0}}. \quad (3)$$

Under the constraints $\theta_2 = \theta_1 + \alpha$ and $\theta_4 = \theta_3 + \beta$, the Lagrangian becomes a function of six variables,

$$L(\dot{\theta}_1, \dot{\theta}_3, \dot{\alpha}, \dot{\beta}, \alpha, \beta) = T(\dot{\theta}_1, \dot{\theta}_3, \dot{\alpha}, \dot{\beta}) - V(\alpha, \beta). \quad (4)$$

The four equations of motion are then obtained from Lagrange's equations,

$$\frac{d}{dt} \frac{\partial L}{\partial \dot{q}_i} - \frac{\partial L}{\partial q_i} = 0, \quad (5)$$

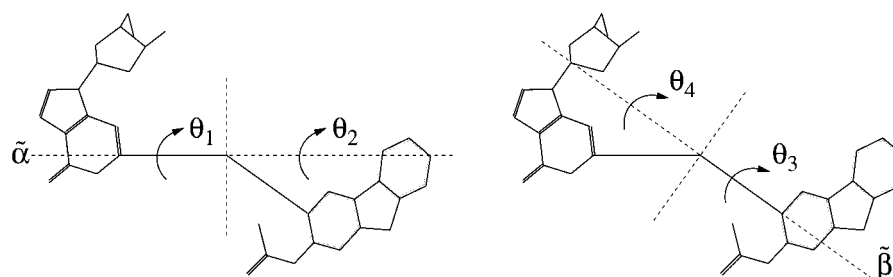


Figure 4. Definitions of the coordinates used in the Lagrangian. The torsion angles are $\alpha = \theta_2 - \theta_1$ and $\beta = \theta_4 - \theta_3$. The corresponding moments of inertia are I_1 : dG about $\tilde{\alpha}$; I_2 : AAF about $\tilde{\alpha}$; I_3 : AAF about $\tilde{\beta}$; I_4 : dG about $\tilde{\beta}$.

where $q_i = \{\theta_1, \theta_3, \alpha, \beta\}$. The coordinates θ_1 and θ_3 are ignorable, and the two Lagrange equations for $q = \theta_1$ and $q = \theta_3$ give the conservation of angular momentum of the free molecule about the two rotation axes. The other two equations give

$$I_\alpha \ddot{\alpha} = - [V_{\alpha\alpha}(\alpha - \alpha_0) + V_{\alpha\beta}(\beta - \beta_0)] \quad (6)$$

$$I_\beta \ddot{\beta} = - [V_{\alpha\beta}(\alpha - \alpha_0) + V_{\beta\beta}(\beta - \beta_0)], \quad (7)$$

where I_α and I_β are the reduced moments of inertia,

$$I_\alpha = \frac{I_1 I_2}{I_1 + I_2}, \quad I_\beta = \frac{I_3 I_4}{I_3 + I_4}. \quad (8)$$

By using harmonic solutions of the form $\alpha - \alpha_0 = \text{Re}[A \exp(-i\omega t)]$ and $\beta - \beta_0 = \text{Re}[B \exp(-i\omega t)]$, the differential equations (6) and (7) are transformed to two homogeneous algebraic equations. Non-trivial solutions are found by setting the secular determinant to zero:

$$\begin{vmatrix} V_{\alpha\alpha} - \omega^2 I_\alpha & V_{\alpha\beta} \\ V_{\alpha\beta} & V_{\beta\beta} - \omega^2 I_\beta \end{vmatrix} = 0. \quad (9)$$

The solutions of this equation give the normal frequencies,

$$\omega_\pm^2 = \frac{1}{2} \left[(\omega_\alpha^2 + \omega_\beta^2) \pm \sqrt{(\omega_\alpha^2 - \omega_\beta^2)^2 + 4\omega_{\alpha\beta}^4} \right], \quad (10)$$

where

$$\omega_\alpha^2 = \frac{V_{\alpha\alpha}}{I_\alpha}, \quad \omega_\beta^2 = \frac{V_{\beta\beta}}{I_\beta}, \quad \omega_{\alpha\beta}^2 = \frac{V_{\alpha\beta}}{\sqrt{I_\alpha I_\beta}}. \quad (11)$$

To find the potential energy coefficients $V_{\mu\nu}$, we performed a series of AM1 calculations on a $20^\circ \times 20^\circ$ grid of α and β about the minimum in 1° steps. The coefficients were found by fitting the data to Eq. (2) using the Marquardt-Levenberg algorithm [32]. The moments of inertia were computed from the cartesian coordinates of the atoms in the equilibrium configuration. The normal-mode frequencies f_- and f_+ were then found from Eq. (10). The results are given in Table II.

Table II. Potential energy coefficients, moments of inertia, and frequencies for the local rotational modes of the torsion angles α and β

$V_{\alpha\alpha}$	0.3412 eV/rad ²
$V_{\alpha\beta}$	0.3182 eV/rad ²
$V_{\beta\beta}$	0.6463 eV/rad ²
I_1	3850 u·Å ²
I_2	4583 u·Å ²
I_3	1725 u·Å ²
I_4	7706 u·Å ²
f_-	$1.34 \times 10^{11} \text{ s}^{-1}$
f_+	$3.66 \times 10^{11} \text{ s}^{-1}$

The rate of conversion between the minima is $R = f \exp(-\Delta E_b/kT)$, where f is the attempt frequency and ΔE_b is the barrier height, 5.93 kcal/mol. The torsional normal modes typically have the lowest energy and so will be appreciably excited at $T = 310$ K. According to Figure 3, α and β rotate in opposite directions. This corresponds to the lower frequency antisymmetric mode. Using f_- for f , we find $R = 8.9 \times 10^6 \text{ s}^{-1}$.

The actual reaction path in living double-stranded DNA would be more complicated due to the presence of other atoms in the chain and the solvent ions. However, our calculations give a reasonable estimate of the difference in total energy between the initial and final states and the rotational dynamics of the torsion angles α and β .

4. Summary

We have investigated the interaction of AAF with the molecule deoxyguanosine to understand the energetics of various conformations as a function of six torsion angles using the quantum mechanical semiempirical molecular orbital method AM1. We have obtained the total energy surface over the entire energy plane. We find a global minimum and one local minimum separated by a modest energy barrier. We have determined the relative equilibrium populations of the two minima at body temperature. From a normal-modes analysis we have determined the dynamics of the interaction site, and have computed the rate of conversion between the two stable configurations.

Acknowledgements

The authors would like to thank the Villanova University Information Technologies center for the generous amount of computing time we received. One of us (M.B.) would also like to thank the Dean's Office of the College of Arts and Sciences for its support during this work.

References

1. Nesnow, S., Argus, M., Bergman, H., Chu, K., Frith, C., Helmes, T., McGaughy, R., Ray, V., Slaga, T.J., Tennant, R. and Weisburger, E.: Chemical Carcinogens. A Review and Analysis of the Literature of Selected Chemicals and the Establishment of the Gene-Tox Carcinogen Data Base. The U.S. Environmental Protection Agency Gene-Tox Program, *Mutat. Res.* **185** (1988), 1–195.
2. Kriek, E., Miller, J.A., Juhl, U. and Miller, E.C.: 8-(*N*-2-fluorenylacetamido) Guanosine, an Arylamidation Reaction Product of Guanosine and the Carcinogen *N*-acetoxy-*N*-2-fluorenylacetamide in Neutral Solution, *Biochemistry* **6** (1967), 177–182.
3. Kriek, E.: Persistent Binding of a New Reaction Product of the Carcinogen *N*-hydroxy-*N*-2-acetylaminofluorene with Guanine in Rat Liver DNA *in vivo*, *Cancer Res.* **32** (1972), 2042–2048.
4. Westra, J.G., Kriek, E. and Hittenhausen, H.: Identification of the Persistently Bound Form of the Carcinogen *N*-acetyl-2-aminofluorene to Rat Liver DNA *in vivo*, *Chem. Biol. Interactions* **15** (1976), 149–164.
5. Yamasaki, H., Leffler, S. and Weinstein, I.B.: Effect of *N*-2-acetylaminofluorene Modification on the Structure and Template Activity of DNA and Reconstituted Chromatin, *Cancer Res.* **37** (1977), 684–691.
6. Yamasaki, H., Pulkrabek, P., Grunberger, D. and Weinstein, I.B.: Differential Excision from DNA of the C8 and N2 Guanosine Adducts of *N*-acetyl-2-aminofluorene by Single Strand-Specific Endonucleases, *Cancer Res.* **37** (1977), 3756–3760.
7. Santella, R.M., Grunberger, D., Weinstein, I.B. and Rich, A.: Induction of the Z Conformation in poly(dG-dC).poly(dG-dC) by Binding of *N*-2-acetylaminofluorene to Guanine Residues, *Proc. Natl. Acad. Sci. USA* **78** (1981), 1451–1455.
8. Burnouf, D., Koehl, P. and Fuchs, R.P.P.: Single Adduct Mutagenesis: Strong Effect of the Position of a Single Acetylaminofluorene Adduct within a Mutation Hot Spot, *Proc. Natl. Acad. Sci. USA* **86** (1989), 4147–4151.
9. Gupta, P.K., Pandrangi, R.G., Lee, M.S. and King, C.M.: Induction of Mutations by *N*-acetoxy-*N*-acetyl-2-aminofluorene modified M13 Viral DNA, *Carcinogenesis* **12** (1991), 819–824.
10. Shibutani, S., Suzuki, N. and Grollman, A.P.: Mutagenic Specificity of (acetylamino) Fluorene-derived DNA Adducts in Mammalian Cells, *Biochemistry* **37** (1998), 12034–12041.
11. Irving, C.C. and Veazey, R.A.: Persistent Binding of 2-acetylaminofluorene to Rat Liver DNA *in vivo* and Consideration of the Mechanism of Binding of *N*-hydroxy-2-acetylaminofluorene to Rat Liver Nucleic Acids, *Cancer Res.* **29** (1969), 1799–1804.
12. Kriek, E.: Carcinogenesis by Aromatic Amines, *Biochim. Biophys. Acta* **355** (1974), 177–203.
13. Kriek, E. and Westra, J.G.: Structural Identification of the Pyrimidine Derivatives formed from *N*-(deoxyguanosin-8-yl)-2-aminofluorene in Aqueous Solution at Alkaline pH, *Carcinogenesis* **1** (1980), 459–468.
14. Fuchs, R.P.P. and Daune, M.P.: Physical Studies on Deoxyribonucleic Acid after Covalent Binding of a Carcinogen, *Biochemistry* **11** (1972), 2659–2666.
15. Fuchs, R.P.P. and Daune, M.P.: Dynamic Structure of DNA modified with the Carcinogen *N*-acetoxy-*N*-2-acetylaminofluorene, *Biochemistry* **13** (1974), 4435–4440.

16. Fuchs, R.P.P.: *In Vitro* Recognition of Carcinogen-Induced Local Denaturation Sites Native DNA by S1 Endonuclease from *Aspergillus oryzae*, *Nature* **257** (1975), 151–152.
17. Fuchs, R.P.P., Lefevre, J.F., Pouyet, J. and Daune, M.P.: Comparative Orientation of the Fluorene Residue in Native DNA modified by *N*-acetoxy-*N*-2-acetylaminofluorene and two 7-halogeno Derivatives, *Biochemistry* **15** (1976), 3347–3351.
18. Hingerty, B. and Broyde, S.: Conformation of the Deoxydinucleoside Monophosphate dCpdG modified at Carbon 8 of Guanine with 2-(acetylamino) Fluorene, *Biochemistry* **21** (1982), 3243–3252.
19. Broyde, S. and Hingerty, B.: Conformation of 2-aminofluorene-modified DNA, *Biopolymers* **22** (1983), 2423–2441.
20. Hingerty, B.E. and Broyde, S.: Energy minimized Structures of Carcinogen-DNA Adducts: 2-acetylaminofluorene and 2-aminofluorene, *J. Biomol. Struct. Dyn.* **4** (1986), 365–372.
21. Shapiro, R., Hingerty, B.E. and Broyde, S.: Minor-groove Binding Models for Acetylaminofluorene modified DNA, *J. Biomol. Struct. Dyn.* **7** (1989), 493–513.
22. Fritsch, V. and Westhof, E.: Minimization and Molecular Dynamics Studies of Guanosine and Z-DNA modified by *N*-2-acetylaminofluorene, *J. Comp. Chem.* **12** (1991), 147–166.
23. Besson, M. and Mihalek, C.L.: Total Energy of Deoxyguanosine bonded to *N*-2-acetylaminofluorene by the Semi-Empirical Modified-Neglect of Differential Diatomic Overlap Method, *Mutat. Res.* **473** (2001), 211–217.
24. Grad, R., Shapiro, R., Hingerty, B.E. and Broyde, S.: A Molecular Mechanics and Dynamics Study of the Minor Adduct between DNA and the Carcinogen 2-(acetylamino) Fluorene (dG-N²-AAF), *Chem. Res. Toxicol.* **10** (1997), 1123–1132.
25. Mitchell, A.D. and Cross, L.C. (eds.): *Tables of Interatomic Distances and Configuration in Molecules and Ions*, Special Pub. No. 11, Chemical Society, London, 1958, p. M237.
26. Neidle, S., Kuroda, R., Broyde, S., Hingerty, B.E., Levine, R.A., Miller, D.W. and Evans, F.E.: Studies on the Conformation and Dynamics of the C8-substituted Guanine Adduct of the Carcinogen Acetylaminofluorene; Model for a Possible Z-DNA modified Structure, *Nucleic Acids Res.* **12** (1984), 8219–8233.
27. Dewar, M.J.S., Zoebisch, E.G., Healy, E.F. and Stewart, J.P.P.: AM1: A New General Purpose Quantum Mechanical Molecular Model, *J. Am. Chem. Soc.* **107** (1985), 3902–3909.
28. Stewart, J.J.P.: MOPAC: A Semiempirical Molecular Orbital Program, *J. Computer-Aided Molecular Design* **4** (1990), 1–105.
29. Dewar, M.J.S. and Thiel, W.: Ground States of Molecules. 38. The MNDO Method. Applications and Parameters, *J. Am. Chem. Soc.* **99** (1977), 4899–4907.
30. Fletcher, R. and Powell, M.J.D.: A Rapidly Convergent Descent Method for Minimization, *Comp. J.* **6** (1963), 163–168.
31. Davidon, W.C.: Variance Algorithm for Minimization, *Comp. J.* **10** (1968), 406–410.
32. Press, W.H., Flannery, B.P., Teukolsky, S.A. and Vetterling, W.T.: *Numerical Recipes*, Cambridge University Press, Cambridge, 1986.